Soliton dynamics in gyrotropic molecular chains

M. T. Primatarowa and K. T. Stoychev
Institute of Solid State Physics, Bulgarian Academy of Sciences, 1784 Sofia, Bulgaria
(Received 20 July 1993; revised manuscript received 30 November 1993)

Envelope solitons formed by anharmonic intramolecular vibrations in gyrotropic molecular chains are investigated. The amplitudes of the circularly polarized modes obey a nonlinear Schrödinger equation which possesses bright- and dark-soliton solutions. The dependence of the solutions on the carrier wavelength and the gyration coefficient is analyzed. Linearly polarized solitons are described by a pair of conjugated circularly polarized pulses whose dynamics is governed by a system of coupled nonlinear Schrödinger equations. The system is studied analytically and numerically and different evolutionary patterns are obtained, corresponding to a coupled or an uncoupled single-soliton solution or a coupled two-soliton solution. The process of collision of circularly polarized solitons is also investigated.

I. INTRODUCTION

Solitary waves (solitons) in one-dimensional molecular chains have been the subject of intensive studies for over two decades. Widely investigated are Davydov-type solitons formed of a vibrational or electronic molecular exciton bound to lattice phonons.[1–12] The influence of the intramolecular anharmonicity on the properties of vibrational solitons has been investigated in Refs. 6 and 11–13. In Refs. 2, 14, and 15 the Pauli character of electronic excitons has been taken into account, resulting in an additional nonlinear exciton-exciton interaction. Vibronic-type solitons formed of electronic and vibrational intramolecular excitations have been studied in Ref. 16. In contrast to the Davydov-type solitons where the interaction with the lattice is essential, solitons formed only of nonlinear intramolecular excitations can be referred to as exciton solitons. Most previous works on solitary waves are restricted to long-wavelength excitations near the center of the Brillouin zone with parabolic dispersion. More complicated dispersion mechanisms have been considered in Refs. 17–19 for the case of lattice solitons and in Ref. 20 for polariton solitons.

The effects of gyrotropy on the optical properties and spectra of crystals both in the visible and in the infrared region have been widely investigated.[21–24] Most common of these are the rotary power dispersion, the circular dichroism, and the eigenmode frequency splitting linear in the wave vector. They have their origin in the lifting of the degeneracy of circularly polarized modes for finite wave vectors. Due to their small values in the optical region (compared to the dimensions of the Brillouin zone) these effects, although observable, are usually small. For larger values of the wave vector a considerable separation between the phonon branches may occur[25,26] which increases the role of gyrotropy. In this paper we examine the effects of gyrotropy on the vibrational soliton dynamics in molecular chains with chiral symmetry. In Sec. II we derive the nonlinear equation which governs the soliton dynamics of circularly polarized modes and analyze the dependence of the solutions on the carrier wave number and the gyration coefficient.

The analysis carried out in Sec. II is the first and necessary step in the investigation of the dynamics of envelope solitons formed of linearly polarized excitations. As it is well known,[21,22,24,27] these excitations are degenerate along the optical axis in uniaxial gyrotropic crystals. The degeneracy is lifted for circular polarizations which diagonalize the linear part of the Hamiltonian. The total Hamiltonian contains also anharmonic terms which describe different nonlinear interactions between the two circular modes and which depend on the symmetry of the system. These terms can be determined from a group-theoretical analysis similar to the one carried out in Ref. 28. In Sec. III, we determine the allowed anharmonic terms in the Hamiltonian for arbitrary cyclic symmetry of the molecules. We derive a system of coupled nonlinear Schrödinger-type equations for the circular vibrational amplitudes and obtain soliton solutions. In Sec. IV we present the results of numerical simulations of the soliton dynamics of a discrete molecular chain and give a criterion for the different types of dynamic behavior. Section V contains some concluding remarks.

II. CIRCULARLY POLARIZED EXCITATIONS

We shall consider a linear chain of molecules possessing n-fold rotation axis along the chain and lacking a center of inversion. The system thus belongs to one of the point groups C_n or D_n and exhibits gyrotropic properties. The Hamiltonian of a system of left *or* right circularly polarized intramolecular vibrations can be written in the Heitler-London approximation in the following way:[21,29]

$$H=\hbar\omega_0\sum_n B_n^\dagger B_n+\sum_{n,m} M_{nm}B_n^\dagger B_m+(g/2)\sum_n B_n^\dagger B_n^\dagger B_n B_n \ , \tag{1}$$

where $\hbar\omega_0$ is the intramolecular excitation energy and $B_n^\dagger$ (B_n) are the corresponding creation (annihilation) Bose operators (for simplicity we consider chains with one molecule per unit cell and take into account one vibrational mode of the molecule). The second term in (1) describes the resonant intermolecular interaction (M_{nm} are

the corresponding matrix elements) responsible for the exciton dispersion. The last term in (1) describes the nonlinear interaction between the vibrational excitons associated with the quartic anharmonicity. To a very good approximation this interaction can be considered local and hence only diagonal nonlinear terms are taken into account. The intramolecular excitations have usually narrow energy bands ($|M_{nm}| \ll \hbar\omega_0$) and only terms conserving the number of particles are kept.

The equation of motion for the operator B_n yields

$$i\hbar\frac{\partial}{\partial t}B_n=\hbar\omega_0 B_n+\sum_m M_{nm}B_m+gB_n^{\dagger}B_nB_n \ . \tag{2}$$

In gyrotropic systems the matrix elements M_{nm} have a nonzero imaginary antisymmetric part, in addition to the symmetric one ($M_{nm}=M_{nm}^{s}+iM_{nm}^{as}$, $M_{nm}^{s}=M_{mn}^{s}$, $M_{nm}^{as}=-M_{mn}^{as}$). M_{nm}^{s} characterizes the resonant dipole-dipole interaction between the molecules, while M_{nm}^{as} is associated with the dipole-quadrupole interaction which is different for intermolecular exchange of left and right circularly polarized excitations.[28,29] The matrix elements M_{nm}^{s} and M_{nm}^{as} depend in general on the molecules' displacements from equilibrium, but in order to simplify the analysis and to study the intrinsic properties of exciton solitary waves we shall consider only the case of fixed molecules. The presence of lattice phonons and the exciton-phonon interaction leads to an additional (indirect) interaction between the excitons, the effect of which can be included in the anharmonicity constant g.

For a linear chain with one molecule per unit cell and nearest-neighbor interaction the nonvanishing matrix elements can be represented as

$$\begin{aligned} &M_{nn+1}^{s}=M_{n+1n}^{s}=M \ , \\ &M_{nn+1}^{as}=-M_{n+1m}^{as}=\mp\gamma \ , \quad M,\gamma-\text{real} \ , \end{aligned} \tag{3}$$

where the two signs in front of γ correspond to excitations with different handedness.

As the intramolecular vibrations obey Bose statistics and an arbitrary number of excitations can be localized on one molecule, the averaging of Eq. (2) can be carried out with the help of a wave function involving on-site coherent states[30,11,12]

$$\begin{aligned} &|\Psi(t)\rangle=\prod_n|\beta_n(t)\rangle \ , \\ &|\beta_n(t)\rangle\equiv\exp[-\tfrac{1}{2}|\beta_n(t)|^2]\exp[\beta_n(t)B_n^{\dagger}]|0\rangle \ , \end{aligned} \tag{4}$$

with the property

$$B_n|\beta_n(t)\rangle=\beta_n(t)|\beta_n(t)\rangle \ .$$

This results in the following equation for the amplitudes:

$$\begin{aligned} i\hbar\frac{\partial}{\partial t}\beta_n=&\hbar\omega_0\beta_n+M(\beta_{n+1}+\beta_{n-1}) \\ &\mp i\gamma(\beta_{n+1}-\beta_{n-1})+g|\beta_n|^2\beta_n \ . \end{aligned} \tag{5}$$

We shall consider the case of weak nonlinearities and look for solutions in the form of amplitude-modulated waves with slowly varying envelopes

$$\beta_n(t)=e^{i(kn-\omega t)}\varphi_n(t) \ , \tag{6}$$

where k and ω are the wave number and the frequency of the carrier wave (the lattice constant equals unity). In order to simplify the analysis we shall consider the case when $\varphi_n(t)$ is a real function. Solutions of Eq. (5) corresponding to complex amplitudes have been obtained numerically in Sec. IV, where considerable modifications of the initial envelopes and phases take place. Further we shall employ the semidiscrete approach introduced in Refs. 31, 32, 17, and 18, in which the carrier wave is treated exactly on the basis of the discrete model, while the envelope is determined in the continuum approximation. This removes the restriction for long carrier wavelengths and permits the study of envelope solitons with arbitrary wave numbers inside the Brillouin zone.

Substituting (6) in (5), expanding $\varphi_{n\pm1}(t)$ into Taylor series around $\varphi_n(t)$ and turning to the continuum approximation through $\varphi_n(t)\rightarrow\varphi(x,t)$, we obtain the following nonlinear equation:

$$i\hbar\frac{\partial\varphi}{\partial t}=(\epsilon_k-\hbar\omega)\varphi-ib_k'\frac{\partial\varphi}{\partial x}+b_k\frac{\partial^2\varphi}{\partial x^2}+g\varphi^3 \ , \tag{7}$$

where

$$\begin{aligned} &\epsilon_k=\hbar\omega_0+2b_k \ , \\ &b_k=M\cos k\pm\gamma\sin k \end{aligned} \tag{8}$$

is the energy of the noninteracting excitons and

$$b_k'\equiv\frac{\partial\epsilon_k}{\partial k}=2(-M\sin k\pm\gamma\cos k)$$

is their group velocity. Near the center of the Brillouin zone ($k\ll1$) b_k reduces to

$$b_k=M\pm\gamma k-(M/2)k^2 \ .$$

The term proportional to γ is associated with the gyrotropy and depending on the structure γ can be either positive or negative. In what follows we shall consider $\gamma>0$ and according to the common conventions[33] the upper or lower sign will correspond to excitations with right or left circular polarization. It should be noted that the phase velocity of the right-handed excitations is larger.

In addition to the standard nonlinear Schrödinger equation, Eq. (7) contains also the first spatial derivative of the function. It decomposes into the following pair of differential equations:

$$(\epsilon_k-\hbar\omega)\varphi+b_k\frac{\partial^2\varphi}{\partial x^2}+g\varphi^3=0 \ , \tag{9}$$

$$\hbar\frac{\partial\varphi}{\partial t}=2(M\sin k\mp\gamma\cos k)\frac{\partial\varphi}{\partial x} \ , \tag{10}$$

which determine completely the soliton dynamics.

The nonlinear equation (9) has two types of soliton solutions which depend on the sign of the ratio b_k/g. For $b_k/g>0$, Eq. (9) has a bell-shaped bright-soliton solution [Fig. 1(a)]

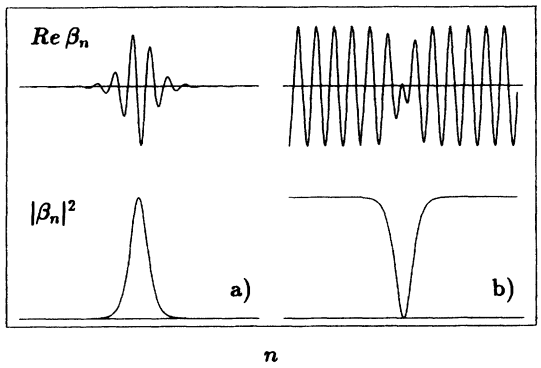

FIG. 1. Envelope soliton solutions. (a) Bright soliton and (b) dark soliton.

$$\varphi(x,t)=\varphi_0 \operatorname{sech}\frac{x-vt}{L} . \tag{11}$$

It corresponds to a pulse of nonlinear excitons with density $\varphi^2(x,t)$ and width $2L$, propagating with a constant velocity v. The substitution of (11) in (9) leads to the following relations between the soliton parameters:

$$\epsilon_k-\hbar\omega+\frac{b_k}{L^2}=0 , \tag{12}$$

$$2\frac{b_k}{L^2}-g\varphi_0^2=0 . \tag{13}$$

Combining (12) and (13), the following expression for the carrier-wave frequency is readily obtained:

$$\omega=\hbar^{-1}(\epsilon_k+g\varphi_0^2/2) . \tag{14}$$

The amplitude φ_0 of the soliton is related to the number of the excitons N_e in the chain through the normalization condition

$$\int_{-\infty}^{\infty}\varphi^2(x,t)dx=2\varphi_0^2L=N_e . \tag{15}$$

From (15) and (13) the following relation for the bell-soliton width holds:

$$L=4b_k/(gN_e) . \tag{16}$$

It is worth mentioning that the slowly varying amplitude condition $L\gg 1$ leads to small nonlinear terms in (9), (12), and (14).

The total energy, stored in the bell soliton calculated from the Hamiltonian (1) with the wave function (4) in the continuum limit is

$$E\equiv\langle\Psi(t)|H|\Psi(t)\rangle=\epsilon_kN_e+\frac{g^2}{48b_k}N_e^3 . \tag{17}$$

In the case when $b_k/g<0$, Eq. (9) has a solution with the shape of a kink (dark soliton) [Fig. 1(b)]

$$\varphi(x,t)=\varphi_1\tanh\frac{x-vt}{L} . \tag{18}$$

This solution corresponds to the formation of a region with a decreased exciton density with a profile $\varphi^2(x,t)$ which propagates with a constant velocity v. The substitution of (18) in (9) leads to the following relations:

$$\omega=\hbar^{-1}(\epsilon_k+g\varphi_1^2) , \tag{19}$$

$$2\frac{b_k}{L^2}+g\varphi_1^2=0 . \tag{20}$$

If we consider a chain with N molecules and N_e excitations (same as in the case of bright solitons), the amplitude φ_1 of the kink can be determined from the normalization condition

$$\int_{-N/2}^{N/2}\varphi^2(x,t)dx=\varphi_1^2(N-2L)=N_e . \tag{21}$$

If the chain is much longer than the width of the dark soliton ($N\gg 2L$), φ_1^2 is approximately equal to the average exciton density in the chain ($\varphi_1^2\approx N_e/N$), which for one and the same N_e is much smaller than the exciton density in the bright soliton φ_0^2. According to (21) and (20), the width of the dark soliton is

$$L=(-2b_kN/gN_e)^{1/2} . \tag{22}$$

If we compare the bright- and dark-soliton solutions corresponding to excitations with equal exciton numbers N_e and wave numbers k, but opposite signs of the intermolecular interactions or the nonlinearity (i.e., opposite sign of the ratio b_k/g), we can see that the width of the dark soliton (22) is much larger than the corresponding bright-soliton width (16) and the nonlinear corrections for the dark soliton are much smaller, i.e., it is in general a much weaker nonlinear formation. The energy of the dark soliton is

$$E\equiv\langle\Psi(t)|H|\Psi(t)\rangle$$
$$=\epsilon_kN_e+gN_e^2/2N+\frac{4b_k}{3}|g/2b_k|^{1/2}(N_e/N)^{3/2} . \tag{23}$$

The second term in (23) gives the main nonlinear correction to the energy, while the last term, which has the opposite sign, can be neglected.

The anharmonicity constant g is usually negative and corresponds to attraction between the excitons, in which case the energy of the bright or dark solitons is lower than the free N_e-exciton energy.

The velocity of both bright and dark solitons determined from Eq. (10) is

$$v=2\hbar^{-1}(-M\sin k\pm\gamma\cos k) \tag{24}$$

and coincides with the group velocity of the excitons. In the long-wave limit ($k\ll 1$) it may be approximated by

$$v=2\hbar^{-1}(\pm\gamma-Mk) .$$

The above results show that the type of the solution and the soliton parameters (velocity and width) depend strongly on the gyration coefficient γ. The type of the solution is determined from the sign of the ratio b_k/g. Being local, the anharmonicity constant g is independent on the wave number. The dispersion coefficient b_k, however, is wave-number dependent (Fig. 2) and within our model it changes sign at a given point inside the Brillouin zone which is the cutoff wave number separating the

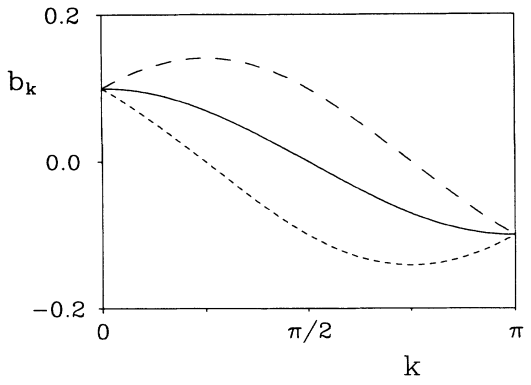

FIG. 2. Exciton disperson curves for $M=0.1$ and $\gamma=0$ (solid line), $\gamma=0.1$ (dashed lines) (b_k, M, and γ measured in units of $\hbar\omega_0$). The long (short) dashed line corresponds to right (left) polarizations.

different soliton solutions. The sign of b_k near the center and near the boundary of the zone is determined from the sign of the symmetric part of the intermolecular interaction M. For intramolecular (optical) phonons M is usually positive, while the anharmonicity constant g is usually negative and thus dark solitons are formed near the center and bright solitons—near the boundary of the Brillouin zone. If one of the quantities g or M changes sign, the bright and dark solitons change places. These results are consistent with the results of Ref. 34.

The presence of gyrotropy influences considerably the cutoff wave number and the soliton parameters. The values and the sign of the soliton velocity (24) near the center and near the boundary of the zone are determined exclusively by the gyration coefficient and in these regions solitons with different handedness will have opposite velocities. Near the cutoff wave number the widths of the solitons go to zero (Fig. 3) while the amplitudes and the energies diverge. In this region, however, the slowly varying amplitude condition is violated and the corresponding solutions may not be valid.

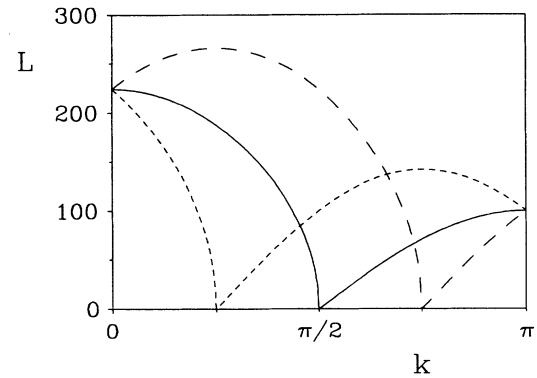

FIG. 3. Width of the solitons (in lattice constants) for $g=0.001$, $N_e=1$, $N=1000$, and $M=0.1$. The solid, long-dashed, and short-dashed curves correspond to those in Fig. 2. The zeros are the cutoff wave numbers separating the bright- and dark-soliton solutions.

III. LINEARLY POLARIZED EXCITATIONS

The transverse linearly polarized intramolecular vibrations in the system can be described in the harmonic approximation by the following Hamiltonian:

$$H_0=\hbar\omega_0\sum_n (a_n^\dagger a_n+b_n^\dagger b_n) + \sum_{n,m}[M^s_{nm}(a_n^\dagger a_m+b_n^\dagger b_m)+M^{as}_{nm}(a_n^\dagger b_m-b_n^\dagger a_m)] , \tag{25}$$

where $\hbar\omega_0$ is the intramolecular excitation energy of the two degenerate modes, and $a_n^\dagger$, a_n and $b_n^\dagger$, b_n are the corresponding creation (annihilation) Bose operators. The antisymmetric matrix elements M^{as}_{nm} mix the two linearly polarized modes and are responsible for the gyrotropic properties of the system.

The Hamiltonian (25) is diagonalized with the help of a transformation to right and left circularly polarized modes with operators $A_n^\dagger$, A_n and $B_n^\dagger$, B_n:

$$A_n=(a_n+ib_n)/\sqrt{2} , \quad B_n=(a_n-ib_n)/\sqrt{2} \tag{26}$$

and takes the form

$$H_0=\hbar\omega_0\sum_n (A_n^\dagger A_n+B_n^\dagger B_n) + \sum_{n,m}[(M^s_{nm}+iM^{as}_{nm})A_n^\dagger A_m+(M^s_{nm}-iM^{as}_{nm})B_n^\dagger B_m] . \tag{27}$$

It can be seen that the intermolecular-interaction terms associated with exchange of right and left circularly polarized vibrations are different and this leads to different phase velocities of the two waves.

The formation of solitons in the system is due to the anharmonicity of the intramolecular vibrations. As these excitations have narrow energy bands, the possible lowest-order nonlinear terms in the Hamiltonian which conserve the number of particles are

$$H_{\rm int}=(g_1/2)\sum_n (A_n^\dagger A_n^\dagger A_n A_n+B_n^\dagger B_n^\dagger B_n B_n) +g_2\sum_n A_n^\dagger B_n^\dagger A_n B_n +(g_3/2)\sum_n (A_n^\dagger A_n^\dagger B_n B_n+B_n^\dagger B_n^\dagger A_n A_n) . \tag{28}$$

The first term ($\sim g_1$) describes the nonlinear interaction between quasiparticles of one and the same type and it governs the formation of left or right circularly polarized solitons. The second and third terms describe the nonlinear interaction between quasiparticles of different types, where the term proportional to g_2 conserves the individual number of particles, while the term proportional to g_3 conserves only the total number of particles. The symmetry-allowed nonlinear terms can be determined from group-theoretical considerations similar to these in Ref. 28.

Using the standard relations between circularly (q_{rm}, q_{lm}) and linearly (q_{xm}, q_{ym}) polarized normal coordi-

nates and the corresponding operators (26) together with the second-quantization form of the linear coordinates

$$q_{xm}=(a_m^\dagger+a_m)/\sqrt{2}\ ,\quad q_{ym}=(b_m^\dagger+b_m)/\sqrt{2} \tag{29}$$

the following relations for the circularly polarized normal coordinates can be obtained:[28]

$$q_{rm}=(A_m+B_m^\dagger)/\sqrt{2}\ ,\quad q_{lm}=(A_m^\dagger+B_m)/\sqrt{2}\ . \tag{30}$$

The normal coordinates q_{rm} and q_{lm} are transformed as the basis functions of a pair of complex conjugated representations of the symmetry point group[35] of the molecules C_n or D_n. For the great majority of molecules $n=1,2,3,4,6$, however, molecules with different n also exist. The generic element of the cyclic point groups has the form $\exp(2\pi i/n)$. The product $q_{rm}q_{lm}$ is invariant for all systems with cyclic or axial symmetry and so are all the powers of this product. Thus the quartic anharmonic term $q_{rm}^2q_{lm}^2$ in the potential energy will always give a nonvanishing contribution and with the help of (30) yields the first two nonlinear terms in (28) with $g_2=2g_1$. If cubic anharmonic terms (which do not conserve the number of particles) are taken into account through the perturbation theory, they lead also to terms of the same type, so in general we can consider $g_2\neq 2g_1$. In molecules belonging to the point groups C_2, D_2, C_4 or D_4, anharmonic terms of the type q_{rm}^4 and q_{lm}^4 are also invariant and they lead to the last term in (28). For all other point groups C_n and D_n (with $n\neq 2,4$) such terms are not allowed and for them $g_3\equiv 0$.

Thus the system of left and right circularly polarized anharmonic excitations in molecular chains with arbitrary chiral symmetry with $n\neq 2,4$ can be described by the following Hamiltonian:[28]

$$\begin{aligned}H=&\hbar\omega_0\sum_n(A_n^\dagger A_n+B_n^\dagger B_n)\\&+\sum_{n,m}[(M_{nm}^s+iM_{nm}^{as})A_n^\dagger A_m+(M_{nm}^s-iM_{nm}^{as})B_n^\dagger B_m]\\&+(g_1/2)\sum_n(A_n^\dagger A_n^\dagger A_nA_n+B_n^\dagger B_n^\dagger B_nB_n)\\&+g_2\sum_n A_n^\dagger B_n^\dagger A_nB_n\ .\end{aligned} \tag{31}$$

In what follows we shall consider this case only and we shall study the soliton dynamics under the influence of the nonlinear terms proportional to g_1 and g_2. The influence of the term proportional to g_3 will be the subject of a future investigation.

The equations of motion for the operators A_n and B_n lead to the following system of coupled nonlinear equations for the averaged vibrational amplitudes $\alpha_n(t)$ and $\beta_n(t)$:

$$\begin{aligned}i\hbar\frac{\partial\alpha_n}{\partial t}=&\hbar\omega_0\alpha_n+M(\alpha_{n+1}+\alpha_{n-1})-i\gamma(\alpha_{n+1}-\alpha_{n-1})\\&+(g_1|\alpha_n|^2+g_2|\beta_n|^2)\alpha_n\\i\hbar\frac{\partial\beta_m}{\partial t}=&\hbar\omega_0\beta_n+M(\beta_{n+1}+\beta_{n-1})+i\gamma(\beta_{n+1}-\beta_{n-1})\\&+(g_1|\beta_n|^2+g_2|\alpha_n|^2)\beta_n\ ,\end{aligned} \tag{32}$$

where M and γ are the nearest-neighbor intermolecular interaction constants defined in (3). As in the previous section, we shall look for solutions in the form of slowly varying amplitude-modulated waves

$$\alpha_n(t)=e^{i(k_1n-\omega_1t)}\varphi_n(t)\ ,\quad \beta_n(t)=e^{i(k_2n-\omega_2t)}\psi_n(t) \tag{33}$$

and employ again the semidiscrete approximation. The real parts of Eqs. (32) lead to the following system of coupled nonlinear equations:

$$\begin{aligned}&(\epsilon_1-\hbar\omega_1)\varphi+b_1\frac{\partial^2\varphi}{\partial x^2}+(g_1\varphi^2+g_2\psi^2)\varphi=0\\&(\epsilon_2-\hbar\omega_2)\psi+b_2\frac{\partial^2\psi}{\partial x^2}+(g_1\psi^2+g_2\varphi^2)\psi=0\ ,\end{aligned} \tag{34}$$

where

$$\epsilon_{1,2}=\hbar\omega_0+2b_{1,2}\ ,\quad b_{1,2}=M\cos k_{1,2}\pm\gamma\sin k_{1,2}\ . \tag{35}$$

The velocities of the solitons can be determined from the imaginary parts of Eqs. (32):

$$\begin{aligned}\hbar\frac{\partial\varphi}{\partial t}=&2(M\sin k_1-\gamma\cos k_1)\frac{\partial\varphi}{\partial x}\ ,\\\hbar\frac{\partial\psi}{\partial t}=&2(M\sin k_2+\gamma\cos k_2)\frac{\partial\psi}{\partial x}\ .\end{aligned} \tag{36}$$

In the following part of this work we shall concentrate on the bright-soliton solutions which are of greater physical interest. The terms proportional to g_2 describe the nonlinear interactions between the two types of excitations and they influence the soliton dynamics only when the two pulses overlap. For this reason and in order to study the evolution of a linearly polarized pulse we shall pay special attention to the case when the initial conditions for the two pulses are identical. For vanishing g_2 the nonlinear equations (32) are uncoupled and their solutions correspond to noninteracting left and right circularly polarized solitons whose properties were studied in the previous section. If the initial carrier wave numbers are equal ($k_1=k_2$), the solitons will propagate with different frequencies, widths, and velocities in accordance with Eqs. (14), (13), and (24).

An exact analytical solution of Eqs. (32) with nonvanishing g_2 can be obtained if the two solitons coincide and have equal velocities and widths. The bright-soliton solution has the form

$$\varphi(x,t)=\varphi_0\operatorname{sech}\frac{x-vt}{L}\ ,\quad \psi(x,t)=\psi_0\operatorname{sech}\frac{x-vt}{L} \tag{37}$$

and yields the following relations between the solitons parameters:

$$\begin{aligned}&k_2=k_1+2\arctan(-\gamma/M)\ ,\quad b_1=b_2=b\ ,\quad \epsilon_1=\epsilon_2=\epsilon\ ,\\&\omega_1=\omega_2=\hbar^{-1}(\epsilon+b/L^2)\ ,\quad \psi_0^2=\varphi_0^2=\frac{2b}{L^2(g_1+g_2)}\ ,\\&v=-2\hbar^{-1}(M\sin k_1-\gamma\cos k_1)\\&\ =-2\hbar^{-1}(M\sin k_2+\gamma\cos k_2)\ .\end{aligned} \tag{38}$$

Equations (37) and (38) describe a coupled single-

soliton solution with identical envelope functions $\varphi(x,t)\equiv\psi(x,t)$ and different carrier wavelengths. The type of the solution depends on the values of the coefficients in Eqs. (32) and on the initial conditions. The uncoupled (11)–(13) or the coupled (37) and (38) single-soliton solutions hold for corresponding identical initial conditions. If the initial conditions are different from (11)–(13) or (37) and (38), then other solutions are also possible, like many-soliton solutions, periodic solutions and combinations of them. A linearly polarized pulse is equivalent to two conjugated circularly polarized pulses with identical envelopes and phases and in the presence of gyrotropy its initial amplitude distribution does not correspond exactly to any of the solutions (11)–(13) or (37) and (38). The possible evolutionary patterns of such a pulse for different values of the parameters are studied numerically in the next section.

IV. NUMERICAL RESULTS

We have studied the dynamics of two conjugated circularly polarized soliton pulses on a discrete chain, solving numerically Eqs. (32) with periodic boundary conditions. The highly stable Adams predictor-corrector method[36] has been employed with variable order and integration step, adjusted to the local error. We have considered the case of positive effective mass of the excitations ($M<0$) and negative (attractive) nonlinear interactions ($g_{1,2}<0$). The results will hold also for $M>0$ and $g_{1,2}>0$. As initial distribution we have chosen the bright-soliton solution corresponding to $g_2=0$ and $\gamma=0$. The first several examples (Figs. 4–7) reveal the evolution of a linearly polarized pulse, described by two conjugated circularly polarized pulses with initially identical envelopes and carrier wave numbers, launched at the same place in the chain. The last example (Fig. 8) shows the process of collision of conjugated circularly polarized pulses launched at different places in the chain. In all cases the widths of the pulses are of the order of ten lattice constants, so that both the slowly varying amplitude condition is fulfilled ($L\gg1$) and the boundary effects are eliminated ($L\ll N$). The precision of the calculations has been controlled through the conservation of the number of particles with deviations below 10^{-5} for the time intervals under study.

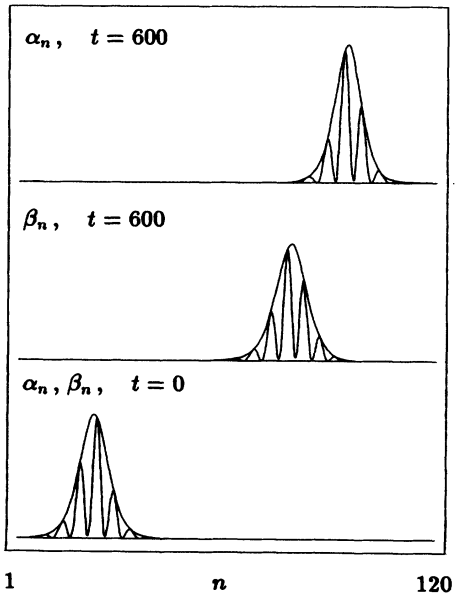

FIG. 4. Time evolution of weakly interacting bright solitons with $k=0.6$, $M=-0.1$, $\gamma=0.01$, $g_1=-0.005$, and $g_2=-0.001$. Plotted are the squared real parts and the squared envelopes of the amplitudes.

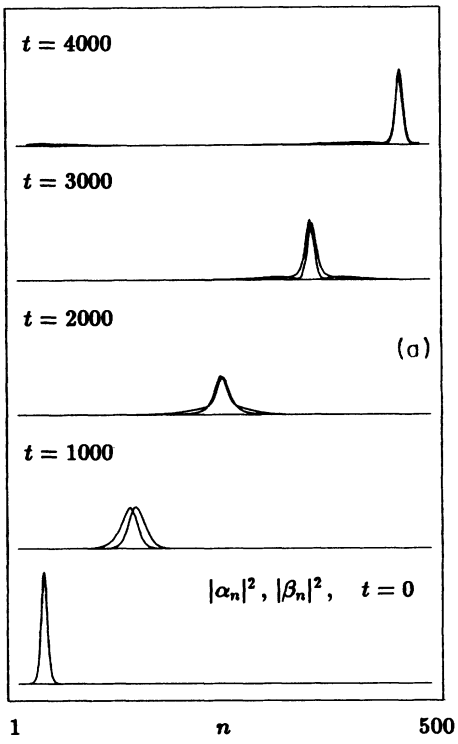

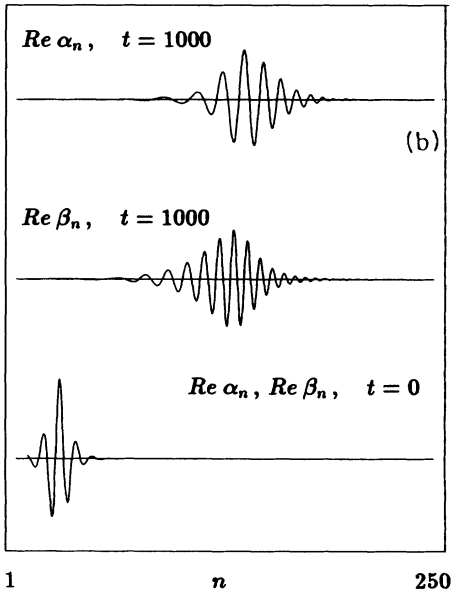

FIG. 5. Coupled propagation of interacting solitons with $k=0.6$, $\gamma=0.01$, and $g_2=-0.005$. (a) Squared envelopes. (b) Real parts.

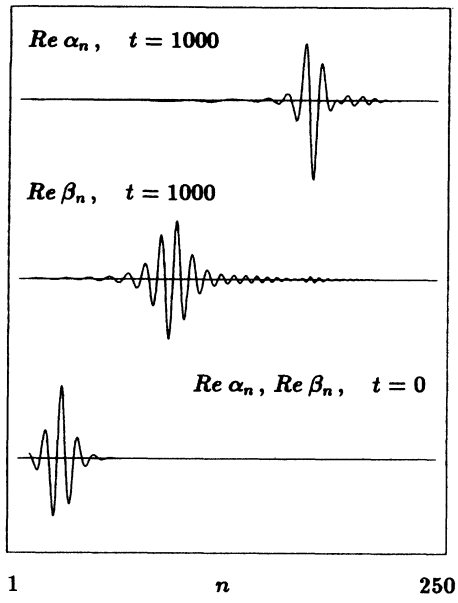

FIG. 6. Uncoupled propagation of interacting solitons with $k=0.6$, $\gamma=0.03$, and $g_2=-0.005$.

$\hbar\omega_0$ scales the energies and ω_0^{-1} — the time.

Figure 4 illustrates the evolution of two weakly interacting ($g_2=-0.001$) right and left circularly polarized solitons. The solution corresponds to the uncoupled propagation of noninteracting solitons described in Sec. II. The two pulses conserve the values of initial wave number and the individual exciton numbers N_e (equal to the surface under the squared envelopes). The presence of gyrotropy leads to different values of the dispersion coefficient b_k (8) and hence to different velocities (24), widths (16), and amplitudes (15). The values of these parameters obtained numerically deviate less than 2% from the theoretical ones.

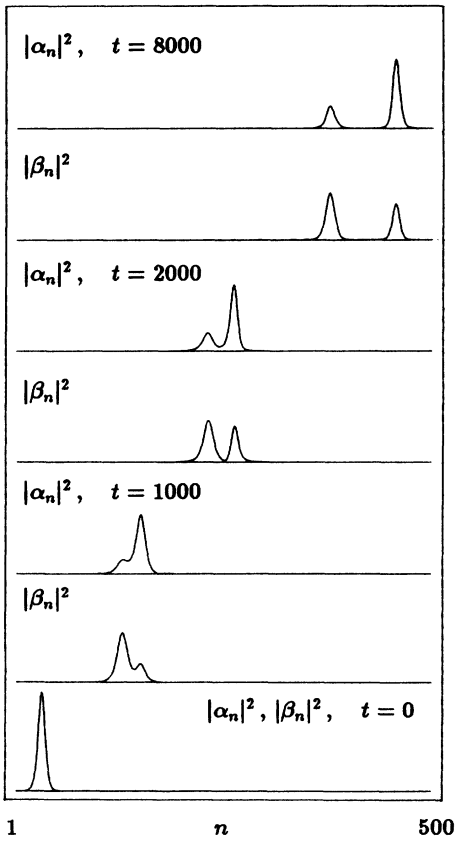

FIG. 7. Coupled two-soliton solution for $k=0.6$, $\gamma=0.015$, and $g_2=-0.005$.

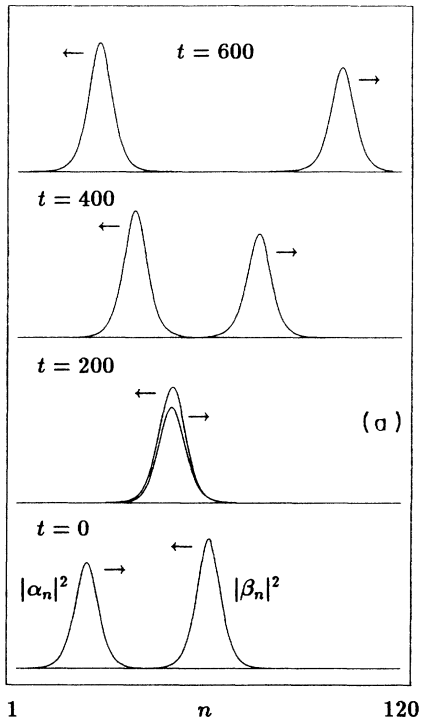

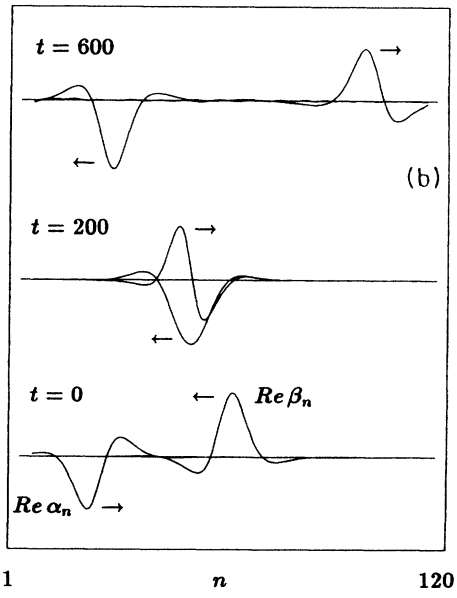

FIG. 8. Collision of interacting solitons with $k=0.2$, $\gamma=0.05$, and $g_2=-0.02$. (a) Squared envelopes. (b) Real parts of the amplitudes.

Larger values of $|g_2|$ (Fig. 5) lead to a coupled motion of the two solitons described asymptotically by the analytical solution (37). The process of coupling of the two pulses can be monitored from Fig. 5(a). As the two pulses have different initial velocities, they start to move separately until the nonlinear interaction g_2 pulls them together. This process is accompanied by an emission of about $\frac{1}{4}$ of the total number of the excitons into plane-wave trains from the front or rear tail of the pulses. After $T=4000$ the shape of the pulses practically does not change. The velocity and the final shape of the two coupled solitons agree within 1% with these obtained from (38) for the reduced exciton number. The carrier wave numbers of the two pulses are modified according to (38) and one becomes smaller and the other—larger than the initial wave number [Fig. 5(b)]. It is interesting to note, that (i) the modification of the wave numbers takes place at an early stage of the process of coupling of the pulses ($t=1000$), before the final adjustment of the envelopes, and (ii) the wave numbers and hence the velocities of the tails are different from these in the central part of the pulses and this is the cause for the emission of plane waves.

An increase of the gyration coefficient ($\gamma=0.03$, Fig. 6) leads again to an uncoupled propagation of the two solitons. The wave numbers in the central part of the pulses are equal and the shape of the solitons is similar to the one in Fig. 4. The influence of g_2, however, may be noticed in several minor effects: (i) asymmetric front and rear tails of the solitons; (ii) different wave number of the tails; and (iii) different velocities of the solitons compared to these for $g_2=0$.

The two types of dynamic behavior depend on the balance between the kinetic energy of the relative motion of the solitons related to the gyration coefficient γ and the nonlinear (potential) energy of their interaction which is proportional to g_2. Neglecting small nonlinear corrections, the effective masses of the solitons can be written as

$$m_s=N_e m_{ex}=-\frac{N_e}{2(M\cos k\pm\gamma\sin k)}\ , \tag{39}$$

where the k-dependent exciton effective mass (m_{ex}) is defined as the inverse second derivative of the energy (8). The reduced mass which describes the relative motion of the two solitons is

$$\mu=-\frac{N_e}{4M\cos k}\ . \tag{40}$$

The kinetic energy of the relative motion of the solitons is $\mu\Delta v^2/2$ and the potential energy of their interaction $|g_2|N_e$. The difference in the velocity of left and right circularly polarized solitons with equal carrier wave numbers according to formula (24) is $\Delta v=4\gamma\cos k$. The two solitons will couple if the potential energy exceeds the kinetic one which yields the condition

$$R=\left|\frac{2\gamma^2\cos k}{g_2 M}\right|<1\ . \tag{41}$$

If the opposite inequality holds, the two solitons will be uncoupled. The values of R for the parameters used in Figs. 4, 5, and 6 are 1.65, 0.33, and 2.97, respectively, which explains the observed dynamics.

The criterion (41) gives only a rough estimate of the behavior of the system and it works better for stronger inequalities. This is due to the fact that the solitons are not rigid point masses as assumed above but, rather finite-size deformable objects. In the intermediate region ($R\sim 1$) the picture gets more complicated. Figure 7 illustrates the evolution of the system for $g_2=-0.005$ and $\gamma=0.015$ ($R=0.74$). The amplitude distribution in this case can be classified as a coupled two-soliton solution. There are two pairs of conjugated solitons coupled to each other which move with different velocities. A considerable asymmetry in the amplitudes is also observed. The relative velocity of the two pairs is constant and equal to 0.1, which is five times smaller than the relative velocity of the uncoupled single-soliton solution corresponding to $\gamma=0.015$ and $g_2=0$. With the increase of γ and the decrease of g_2 the asymmetry of the two-soliton solution increases and it turns into an uncoupled single-soliton solution. A more careful observation of the results in Fig. 6 reveals that it is in fact a strongly asymmetric coupled two-soliton solution with deviations 4–5% in the amplitudes and 3–9% in the velocities, compared to the single-soliton solution.

The three types of nonlinear dynamic behavior of the system, which we have obtained, correspond to different physical situations. As the two initial circularly polarized pulses are identical to a single pulse with a linear polarization, the above results show, that for weak gyrotropy and strong nonlinear interaction $|g_2|$ the linearly polarized pulse propagates as a single pulse with a rotating plane of polarization, while in the case of strong gyrotropy and weak nonlinear interaction it decomposes into a pair of left and right circularly polarized solitons moving with different velocities. In the intermediate region, where the kinetic energy of the relative motion is comparable to the potential energy of the soliton interaction, the initial pulse decomposes into a pair of elliptically polarized pulses, propagating with different velocities.

We investigated also the stability of left and right circularly polarized solitons against collision. The two solitons have smaller wave numbers $k=0.2$ and due to the strong gyrotropy ($\gamma=0.05$) have opposite velocities. The difference in their momenta in this case is quite large and even a considerable nonlinear interaction ($|g_2|=0.02$) does not lead to coupling of the solitons. The shape of the envelopes practically does not change during or after the collision [Fig. 8(a)]. However, when the solitons overlap, a strong phase modulation takes place [Fig. 8(b)]. Thus the wavelength of β increases, while the wavelength of α decreases and Reα acquires an additional zero. For larger values of $|g_2|$ the collision of the solitons is accompanied by a noticeable broadening and a decrease of their amplitudes, and they regain their initial shape after longer time intervals.

V. CONCLUSION

We have investigated the dynamics of a circularly and linearly polarized envelope solitons in gyrotropic molecu-

lar chains. In the first part of this paper we have elucidated the properties of solitons formed of left *or* right circularly polarized excitations. We have employed the semidiscrete approximation in which the exciton carrier wave is treated exactly and we have studied envelope solitons with arbitrary values of the wave number. We have shown that the system possesses bright- and dark-soliton solutions, located in different regions of the Brillouin zone and we have determined the soliton parameters such as energy, velocity, width, and amplitude.

Linearly polarized solitons are treated in the second part of this paper as an equivalent pair of left and right circularly polarized pulses with nonlinear interactions between them. A group-theoretical analysis yields the allowed nonlinear terms in the Hamiltonian for the different point groups of symmetry. We have considered molecules possessing n-fold rotation axis with $n \neq 2,4$, in which case there is no energy transfer between the solitons. The presence of gyrotropy tends to separate the pulses, while an attractive nonlinear interaction tends to keep them together. The balance between the kinetic energy of the relative motion of the solitons and the potential energy of their interaction gives the possible evolutionary patterns: a coupled or uncoupled single-soliton solution when stronger inequalities hold, and a coupled two-soliton solution in the intermediate region where the kinetic energy is nearly equal to the potential one. Our results show, that for weak gyrotropy and strong anharmonicity the initial pulse will propagate as a single linearly polarized pulse with a rotating plane of polarization, while in the opposite case it will decompose into two separate circularly polarized pulses moving with different velocities. In the intermediate case the initial pulse will decompose into a pair of elliptically polarized pulses.

We have investigated also the process of collision of right and left circularly polarized solitons. Up to large values of the nonlinear coupling constant the solitons remain stable after the collision, while during the overlapping a phase modulation and a broadening of the solitons takes place.

ACKNOWLEDGMENTS

We are indebted to Professor V. M. Agranovich for suggesting a similar investigation once, and to Professor I.J. Lalov and Professor D.I. Pushkarov for the helpful discussions. This work was supported in part by the National Science Foundation of Bulgaria.

[1]A. S. Davydov and N. I. Kislukha, Phys. Status Solidi B **59**, 465 (1973).
[2]W. Weidlich and W. Heudorfer, Z. Phys. **268**, 133 (1974).
[3]A. S. Davydov and N. I. Kislukha, Phys. Status Solidi B **75**, 735 (1976).
[4]A. S. Davydov, Usp. Fiz. Nauk **138**, 603 (1982) [Sov. Phys. Usp. **25**, 898 (1982)].
[5]S. Takeno, Prog. Theor. Phys. **71**, 395 (1984).
[6]S. Takeno, Prog. Theor. Phys. **73**, 853 (1985).
[7]A. S. Davydov, *Solitons in Molecular Systems* (Reidel, Boston, 1985).
[8]D. W. Brown, K. Lindenberg, and B. J. West, Phys. Rev. A **33**, 4104 (1986).
[9]D. W. Brown, B. J. West, and K. Lindenberg, Phys. Rev. A **33**, 4110 (1986).
[10]X. Wang, D. W. Brown, K. Lindenberg, and B. J. West, Phys. Rev. A **37**, 3557 (1988).
[11]X. Wang, D. W. Brown, and K. Lindenberg, Phys. Rev. B **39**, 5366 (1989).
[12]S. Takeno, J. Phys. Soc. Jpn. **59**, 3127 (1990).
[13]M. T. Primatarowa, Phys. Status Solidi B **138**, 101 (1986).
[14]V. I. Kruglov, J. Phys. C **16**, 5083 (1983).
[15]S. Takeno, Prog. Theor. Phys. **69**, 1798 (1983).
[16]Kh. I. Pushkarov and M. T. Primatarowa, Phys. Status Solidi B **133**, 253 (1986).
[17]N. Flitzanis, St. Pnevmatikos, and M. Remoissenet, J. Phys. C **18**, 4603 (1985).
[18]St. Pnevmatikos, N. Flitzanis, and M. Remoissenet, Phys. Rev. B **33**, 2308 (1986).
[19]D. Hochstrasser, F. G. Mertens, and H. Büttner, Phys. Rev. A **40**, 2602 (1989).
[20]K. T. Stoychev and M. T. Primatarowa, Phys. Rev. B **46**, 10 727 (1992).
[21]V. M. Agranovich, *Theory of Excitons* (Nauka, Moscow, 1968).
[22]V. M. Agranovich and V. L. Ginzburg, *Crystal Optics with Spatial Dispersion and Excitons* (Springer, Berlin, 1984).
[23]G. D. Mahan and J. J. Hopfield, Phys. Rev. **135**, A428 (1964).
[24]A. S. Pine and G. Dresselhaus, Phys. Rev. **188**, 1489 (1969).
[25]M. Hulin, J. Phys. Chem. Solids, Suppl. **21**, 135 (1965).
[26]M. M. Elcombe, Proc. Phys. Soc. (London) **91**, 947 (1967).
[27]D. L. Portigal and E. Burstein, Phys. Rev. **170**, 673 (1968).
[28]I. J. Lalov and J. N. Kotzev, J. Chem. Phys. **89**, 3454 (1988).
[29]I. J. Lalov, J. Chem. Phys. **80**, 1069 (1984).
[30]R. J. Glauber, Phys. Rev. **131**, 2766 (1963).
[31]A. A. Eremko and A. I. Sergienko, Fiz. Tverd. Tela (Leningrad) **24**, 3720 (1982) [Sov. Phys. Solid State **24**, 2122 (1982)].
[32]M. Remoissenet, Phys. Rev. B **33**, 2386 (1986).
[33]J. F. Nye, *Physical Properties of Crystals* (Oxford University Press, Oxford, 1957).
[34]D. I. Pushkarov and M. T. Primatarowa, Phys. Scr. **39**, 620 (1989).
[35]D. L. Landau and E. M. Lifschits, *Quantum Mechanics* (Nauka, Moscow, 1989).
[36]L. F. Shampine and M. K. Gordon, *Computer Solution of Ordinary Differential Equations* (Freeman, San Francisco, 1975).